27. Jacque, J.M., K. Triques, and M. Stevenson, Modulation of HIV-1 replication by RNA interference. *Nature*, 2002. **418**(6896): p. 435-8.
28. Lee, N.S., et al., Expression of small interfering RNAs targeted against HIV-1 rev transcripts in human cells. *Nature Biotechnology*, 2002. **20**(5): p. 500-5.
29. Kapadia, S.B., A. Brideau-Andersen, and F.V. Chisari, Interference of hepatitis C virus RNA replication by short interfering RNAs. *Proceedings of the National Academy of Sciences of the United States of America*, 2003. **100**(4): p. 2014-8.
30. Yokota, T., et al., Inhibition of intracellular hepatitis C virus replication by synthetic and vector-derived small interfering RNAs. *EMBO Reports*, 2003. **4**(6): p. 602-8.
31. Holmes, K.V., Coronaviruses. *Fields' Virology(eds. Knipe, D., et al)*, 2001: p. 1187-1203.
32. Wege, H., S. Siddell, and V. ter Meulen, The biology and pathogenesis of coronaviruses. *Current Topics in Microbiology & Immunology*, 1982. **99**: p. 165-200.
33. Rota, P.A., et al., Characterization of a novel coronavirus associated with severe acute respiratory syndrome. *Science*, 2003. **300**(5624): p. 1394-9.
34. Marra, M.A., et al., The Genome sequence of the SARS-associated coronavirus. *Science*, 2003. **300**(5624): p. 1399-404.
35. Lai, M.M., SARS virus: the beginning of the unraveling of a new coronavirus. *Journal of Biomedical Science*, 2003. **10**(6 Pt 2): p. 664-75.
36. Zeng, F.Y., et al., The complete genome sequence of severe acute respiratory syndrome coronavirus strain HKU-39849 (HK-39). *Experimental Biology & Medicine*, 2003. **228**(7): p. 866-73.
37. Vennema, H., et al., Intracellular transport of recombinant coronavirus spike proteins: implications for virus assembly. *Journal of Virology*, 1990. **64**(1): p. 339-46.
38. Li, W., et al., Angiotensin-converting enzyme 2 is a functional receptor for the SARS coronavirus. *Nature*, 2003. **426**(6965): p. 450-4.
39. Xiao, X., et al., The SARS-CoV S glycoprotein: expression and functional characterization. *Biochemical & Biophysical Research Communications*, 2003. **312**(4): p. 1159-64.
40. Thiel, V., et al., Mechanisms and enzymes involved in SARS coronavirus genome expression. *Journal of General Virology*, 2003. **84**(Pt 9): p. 2305-15.
41. Snijder, E.J., et al., Unique and conserved features of genome and proteome of SARS-coronavirus, an early split-off from the coronavirus group 2 lineage. *Journal of Molecular Biology*, 2003. **331**(5): p. 991-1004.
42. Gao, F., et al., Prediction of proteinase cleavage sites in polyproteins of coronaviruses and its applications in analyzing SARS-CoV genomes. *FEBS Letters*, 2003. **553**(3): p. 451-6.
43. Sawicki, S.G. and D.L. Sawicki, A new model for coronavirus transcription. *Advances in Experimental Medicine & Biology*, 1998. **440**: p. 215-9.
44. Lai, M.M. and D. Cavanagh, The molecular biology of coronaviruses. *Advances in Virus Research*, 1997. **48**: p. 1-100.
45. Li, T., et al., siRNA targeting the leader sequence of SARS-CoV inhibits virus replication. *Gene Therapy*, 2005. **12**(9): p. 751-61.
46. Zheng, B.J., et al., Prophylactic and therapeutic effects of small interfering RNA targeting SARS-coronavirus. *Antiviral Therapy*, 2004. **9**(3): p. 365-74.

47. Shi, Y., et al., Inhibition of genes expression of SARS coronavirus by synthetic small interfering RNAs. *Cell Research*, 2005. **15**(3): p. 193-200.
48. Lu, A., et al., Attenuation of SARS coronavirus by a short hairpin RNA expression plasmid targeting RNA-dependent RNA polymerase. *Virology*, 2004. **324**(1): p. 84-9.
49. Tao, P., et al., Potent and specific inhibition of SARS-CoV antigen expression by RNA interference. *Chinese Medical Journal*, 2005. **118**(9): p. 714-9.
50. Li, B.J., et al., Using siRNA in prophylactic and therapeutic regimens against SARS coronavirus in Rhesus macaque. *Nature Medicine*, 2005. **11**(9): p. 944-51.
51. Wang, Z., et al., Inhibition of severe acute respiratory syndrome virus replication by small interfering RNAs in mammalian cells. *Journal of Virology*, 2004. **78**(14): p. 7523-7.
52. Zhang, Y., et al., Silencing SARS-CoV Spike protein expression in cultured cells by RNA interference. *FEBS Letters*, 2004. **560**(1-3): p. 141-6.
53. Qin, Z.L., et al., Silencing of SARS-CoV spike gene by small interfering RNA in HEK 293T cells. *Biochemical & Biophysical Research Communications*, 2004. **324**(4): p. 1186-93.
54. Elmen, J., et al., Locked nucleic acid (LNA) mediated improvements in siRNA stability and functionality. *Nucleic Acids Research*, 2005. **33**(1): p. 439-47.
55. Wu, C.J., et al., Inhibition of SARS-CoV replication by siRNA. *Antiviral Research*, 2005. **65**(1): p. 45-8.
56. Ni, B., et al., Inhibition of replication and infection of severe acute respiratory syndrome-associated coronavirus with plasmid-mediated interference RNA. *Antiviral Therapy*, 2005. **10**(4): p. 527-33.
57. He, M.L., et al., Inhibition of SARS-associated coronavirus infection and replication by RNA interference. *Jama*, 2003. **290**(20): p. 2665-6.
58. Zhao, P., et al., Small interfering RNA inhibits SARS-CoV nucleocapsid gene expression in cultured cells and mouse muscles. *FEBS Letters*, 2005. **579**(11): p. 2404-10.
59. Haagmans, B.L., et al., Pegylated interferon-alpha protects type 1 pneumocytes against SARS coronavirus infection in macaques. *Nature Medicine*, 2004. **10**(3): p. 290-3.
60. Shlomai, A. and Y. Shaul, Inhibition of hepatitis B virus expression and replication by RNA interference. *Hepatology*, 2003. **37**(4): p. 764-70.
61. McCaffrey, A.P., et al., Inhibition of hepatitis B virus in mice by RNA interference. *Nature Biotechnology*, 2003. **21**(6): p. 639-44.
62. Hamasaki, K., et al., Short interfering RNA-directed inhibition of hepatitis B virus replication. *FEBS Letters*, 2003. **543**(1-3): p. 51-4.
63. Randall, G. and C.M. Rice, Interfering with hepatitis C virus RNA replication. *Virus Research*, 2004. **102**(1): p. 19-25.
64. Seo, M.Y., et al., Small interfering RNA-mediated inhibition of hepatitis C virus replication in the human hepatoma cell line Huh-7. *Journal of Virology*, 2003. **77**(1): p. 810-2.
65. Hamazaki, H., et al., Inhibition of hepatitis C virus RNA replication by short hairpin RNA synthesized by T7 RNA polymerase in hepatitis C virus subgenomic

replicons. *Biochemical & Biophysical Research Communications*, 2006. **343**(3): p. 988-94.
66. Adelman, Z.N., et al., Sindbis virus-induced silencing of dengue viruses in mosquitoes. *Insect Molecular Biology*, 2001. **10**(3): p. 265-73.
67. Adelman, Z.N., et al., RNA silencing of dengue virus type 2 replication in transformed C6/36 mosquito cells transcribing an inverted-repeat RNA derived from the virus genome. *Journal of Virology*, 2002. 76(24): p. 12925-33.
68. Gitlin, L., S. Karelsky, and R. Andino, Short interfering RNA confers intracellular antiviral immunity in human cells.[see comment]. *Nature*, 2002. **418**(6896): p. 430-4.
69. Ge, Q., et al., RNA interference of influenza virus production by directly targeting mRNA for degradation and indirectly inhibiting all viral RNA transcription. *Proceedings of the National Academy of Sciences of the United States of America*, 2003. **100**(5): p. 2718-23.
70. Hu, W.Y., et al., Inhibition of retroviral pathogenesis by RNA interference. *Current Biology*, 2002. 12(15): p. 1301-11.
71. Capodici, J., K. Kariko, and D. Weissman, Inhibition of HIV-1 infection by small interfering RNA-mediated RNA interference. *Journal of Immunology*, 2002. **169**(9): p. 5196-201.
72. Coburn, G.A. and B.R. Cullen, Potent and specific inhibition of human immunodeficiency virus type 1 replication by RNA interference. *Journal of Virology*, 2002. 76(18): p. 9225-31.
73. Park, W.S., et al., Prevention of HIV-1 infection in human peripheral blood mononuclear cells by specific RNA interference. *Nucleic Acids Research*, 2002. **30**(22): p. 4830-5.
74. Surabhi, R.M. and R.B. Gaynor, RNA interference directed against viral and cellular targets inhibits human immunodeficiency Virus Type 1 replication. *Journal of Virology*, 2002. 76(24): p. 12963-73.
75. Martinez, M.A., et al., Suppression of chemokine receptor expression by RNA interference allows for inhibition of HIV-1 replication.[see comment]. *Aids*, 2002. **16**(18): p. 2385-90.
76. Qin, X.F., et al., Inhibiting HIV-1 infection in human T cells by lentiviral-mediated delivery of small interfering RNA against CCR5. *Proceedings of the National Academy of Sciences of the United States of America*, 2003. **100**(1): p. 183-8.
77. Gaggar, A., et al., Localization of regions in CD46 that interact with adenovirus. *Journal of Virology*, 2005. 79(12): p. 7503-13.
78. Manel, N., et al., The ubiquitous glucose transporter GLUT-1 is a receptor for HTLV. *Cell*, 2003. **115**(4): p. 449-59.
79. Zhang, J., et al., Down-regulation of viral replication by adenoviral-mediated expression of siRNA against cellular cofactors for hepatitis C virus. *Virology*, 2004. **320**(1): p. 135-43.
80. Goh, P.Y., et al., Cellular RNA helicase p68 relocalization and interaction with the hepatitis C virus (HCV) NS5B protein and the potential role of p68 in HCV RNA replication. *Journal of Virology*, 2004. 78(10): p. 5288-98.
81. Nomura, R., et al., Human coronavirus 229E binds to CD13 in rafts and enters the cell through caveolae. *Journal of Virology*, 2004. 78(16): p. 8701-8.

82. Hall, A.H., et al., RNA interference using boranophosphate siRNAs: structure-activity relationships. *Nucleic Acids Research*, 2004. **32**(20): p. 5991-6000.
83. Harborth, J., et al., Sequence, chemical, and structural variation of small interfering RNAs and short hairpin RNAs and the effect on mammalian gene silencing. *Antisense & Nucleic Acid Drug Development*, 2003. **13**(2): p. 83-105.
84. Chiu, Y.L. and T.M. Rana, siRNA function in RNAi: a chemical modification analysis. *Rna-A Publication of the Rna Society*, 2003. 9(9): p. 1034-48.
85. Braasch, D.A., et al., RNA interference in mammalian cells by chemically-modified RNA. *Biochemistry*, 2003. **42**(26): p. 7967-75.
86. Amarzguioui, M., et al., Tolerance for mutations and chemical modifications in a siRNA. *Nucleic Acids Research*, 2003. **31**(2): p. 589-95.
87. Czauderna, F., et al., Structural variations and stabilising modifications of synthetic siRNAs in mammalian cells. *Nucleic Acids Research*, 2003. **31**(11): p. 2705-16.
88. Allerson, C.R., et al., Fully 2'-modified oligonucleotide duplexes with improved in vitro potency and stability compared to unmodified small interfering RNA. *Journal of Medicinal Chemistry*, 2005. **48**(4): p. 901-4.
89. Grunweller, A., et al., Comparison of different antisense strategies in mammalian cells using locked nucleic acids, 2'-O-methyl RNA, phosphorothioates and small interfering RNA. *Nucleic Acids Research*, 2003. **31**(12): p. 3185-93.
90. Soutschek, J., et al., Therapeutic silencing of an endogenous gene by systemic administration of modified siRNAs. *Nature*, 2004. **432**(7014): p. 173-8.
91. Morrissey, D.V., et al., Activity of stabilized short interfering RNA in a mouse model of hepatitis B virus replication. *Hepatology*, 2005. **41**(6): p. 1349-56.

INFECTION AND IMMUNITY, June 2006, p. 3682–3683 Vol. 74, No. 6
0019-9567/06/$08.00+0 doi:10.1128/IAI.01731-05

Isolation of a Human Monoclonal Antibody with Strong Neutralizing Activity against Diphtheria Toxin

Mai Kakita,[1] Tsuyoshi Takahashi,[2] Takako Komiya,[3] Yoshitaka Iba,[4] Takao Tsuji,[2] Yoshikazu Kurosawa,[4]* and Motohide Takahashi[3]

Institute for Antibodies Ltd.,[1] Department of Microbiology,[2] and School of Medicine, Institute for Comprehensive Medical Science,[4] Fujita Health University, Toyoake, Aichi 470-1192, and National Institute of Infectious Diseases, Musashimurayama, Tokyo 208-0011,[3] Japan

Received 21 October 2005/Returned for modification 1 November 2005/Accepted 29 March 2006

We isolated a human monoclonal antibody against diphtheria toxin (DT). It bound to fragment B with a binding activity (K_d) of 3.01 nM. The neutralizing activity assayed by the rabbit skin test was estimated to be 73,600 IU/g. This could be used as a therapeutic drug against DT in place of the traditional equine sera.

Antisera prepared from hyperimmune horse blood are still used as drugs against diphtheria toxin (DT) in emergency situations. Since equine antisera could induce serious side effects such as serum sickness, there is a strong need to develop a human monoclonal antibody (Ab) against DT. DT excreted by *Corynebacterium diphtheriae* has been well characterized (12). It is a single polypeptide chain (M_r, 58,000) composed of two structurally distinct regions with three functional domains and contains a protease-sensitive site. The nicked toxin produced upon limited proteolysis consists of two polypeptides that are held together by a disulfide bond. The NH_2-terminal region, fragment A, catalyzes the transfer of the ADP-ribose moiety from NAD to elongation factor 2 and thus blocks protein synthesis (4). The COOH-terminal region, fragment B, binds to a specific receptor on the cell surface and mediates transfer of fragment A to the cytoplasm (6, 11, 14). DT is lethal for susceptible animals, including humans, in doses of 100 ng/kg or less (12). Mass immunization of children has been performed on a worldwide scale since the 1940s. The degree of immunity to DT in the serum of each person should be critical for determination of susceptibility to diphtheria. There is a good correlation between clinical protection and the presence of serum antitoxin, whether this results from disease or immunization. According to internationally accepted definitions, an antitoxin concentration of less than 0.01 IU/ml indicates susceptibility, 0.01 to 0.09 IU/ml indicates basic protection, and >0.1 IU/ml indicates full protection (2). Once the symptoms of this disease start to appear, the antiserum should be given to the patient as soon as possible. The amount of Abs required for curing is much larger than that required to prevent infection. It ranges from 5,000 to 50,000 IU, depending on the degree of disease progress (2).

A human Ab library was screened with DT and diphtheria toxoid (DTD) as the antigen (Ag) by the panning method (3, 5). DT and DTD were kindly given to us by Kunio Ohkuma (Kaketsuken, Kumamoto, Japan). DTD is inactivated toxin that is used for vaccination. It has been prepared by treatment with formaldehyde (13). The Abs were initially prepared in the form of an Ab fused with truncated cp3 (Fab-cp3) and converted to immunoglobulin G1 (IgG1) (3). In this paper, we report data obtained with IgG. Fifty-five different clones were isolated. Four of them, DTD4, DTD8, DTD10, and DTD76, distinctively showed neutralizing activities. The amino acid sequences of these four clones are shown in Fig. 1. Western blotting with separated fragments A and B indicated that DTD4 and DTD76 bound to fragment B and DTD8 and DTD10 bound to fragment A. The rate constants, and thus the binding constants, of these four clones against DTD and DT were measured with the BIAcore instrument (5) (Table 1). Abs were coupled to the sensor chip, and Ags were injected to avoid the influence of divalency. Clones DTD4, DTD8, and DTD10 bound to DT more strongly than to DTD, whereas DTD76 bound to DTD more strongly than to DT.

In vitro DT-neutralizing activities were estimated by the pH color change method (9, 10). When the cells were metabolically active, the color of the medium changed to yellow. When cellular metabolism was stopped by toxin action, it remained red. Thus, the titration endpoint for anti-DT neutralizing activity was taken at the highest dilution of anti-DT Ab to be tested in the well in which the color of the medium was orange. The results are indicated in the left column of values in Table 2. The antitoxin titers are expressed in international units by comparison with the result obtained with equine sera. The in vivo neutralizing activities of Abs against DT were determined by the rabbit skin test as described previously (1, 7). In brief, DT

TABLE 1. Rate constants (k_a, k_d) and dissociation constant (K_d) of IgG form of Abs with DTD and DT assayed by the BIAcore instrument

Clone	Anti-DTD			Anti-DT		
	k_a (10^4 M^{-1} s^{-1})	k_d (10^{-4} s^{-1})	K_d (10^{-9} M)	k_a (10^4 M^{-1} s^{-1})	k_d (10^{-4} s^{-1})	K_d (10^{-9} M)
DTD4	4.14	8.70	21.2	10.6	3.19	3.01
DTD8	4.99	3.82	7.66	16.2	0.831	0.513
DTD10	8.89	3.76	4.22	8.52	0.243	0.285
DTD76	11.9	2.29	1.93	7.8	4.83	6.19

* Corresponding author. Mailing address: Institute for Comprehensive Medical Science, Fujita Health University, Toyoake, Aichi 470-1192, Japan. Phone: 81-562-93-9387. Fax: 82-562-93-8835. E-mail: kurosawa@fujita-hu.ac.jp.

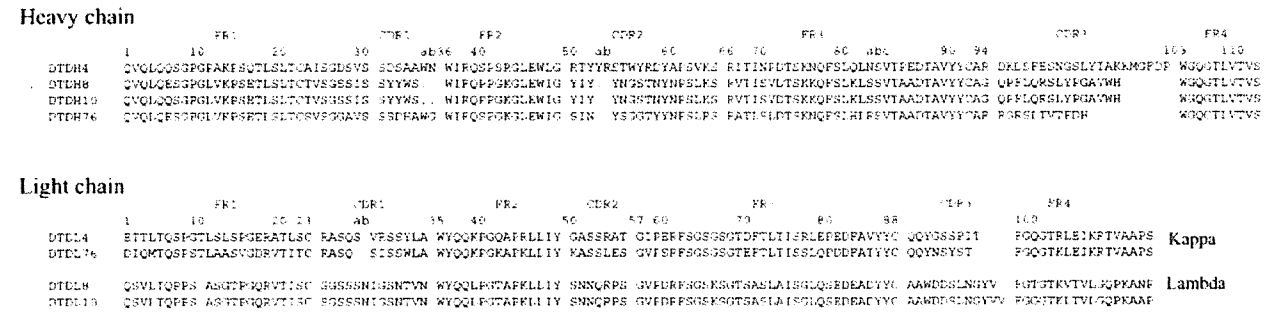

FIG. 1. Amino acid sequences of variable regions of the heavy and light chains of Abs that exhibited neutralizing activities against DT. The numbering of amino acid positions is according to the definition of Kabat et al. (8).

mixed with serially diluted Abs was injected into rabbit back skin. The diameter of local erythema was measured at the site of injection at 48 h postinjection. The results are shown in the rightmost column of Table 2. The antitoxin titers are expressed in international units as relative potency with respect to the result obtained with the standard antitoxin. The neutralizing activities of Abs assayed by the pH color change method and by the rabbit skin test were similar to each other in four cases, indicating a good correlation between the two systems (10).

In the case of DTD4, which showed the strongest neutralizing activity of the four clones, it was estimated to be 73,600 IU/g by the in vivo assay. The binding activity (K_d) with DT was 3.01 nM. On the other hand, while DTD76 bound to DTD with strong affinity, it showed very weak neutralizing activity. Although both clones bound to fragment B, they should recognize completely different epitopes. It is possible that clone DTD4 corresponded to the Ab that had matured in vivo by immunization with vaccine against DT. We propose that DTD4 be clinically tested for therapeutic use.

Nucleotide sequence accession numbers. The nucleotide sequences of the eight genes described in Fig. 1 have been registered in GenBank under accession numbers AB063724 (DTDH4), AB063723 (DTDH8), AB063729 (DTDH10), AB063743 (DTDH76), AB063937 (DTDL4), AB064049 (DTDL76), AB063977 (DTDL8), and AB064205 (DTDL10).

TABLE 2. Neutralizing activity against DT shown by IgG form of Abs

Clone	Neutralizing activity[a]	
	In vitro assay[b]	In vivo assay[c]
DTD4	52,000	73,600
DTD8	4,800	3,360
DTD10	2,300	1,612
DTD76	215	372

[a] In international units per gram.
[b] Measured by the pH color change method.
[c] Measured by the rabbit skin test.

Editor: J. B. Bliska

We thank Kunio Ohkuma and Eisuke Mekada for providing materials. We also thank Atsuko Suzuoki for preparation of the manuscript.

This study was supported in part by a grant for Research on Pharmaceutical and Medical Safety from the Ministry of Health, Labor, and Welfare of Japan.

REFERENCES

1. **Barile, M. F., R. W. Kolb, and M. Pittman.** 1971. United States standard diphtheria toxin for the Schick test and the erythema potency assay for the Schick test dose. Infect. Immun. 4:295–306.
2. **Galazka, A. M.** 1993. Expanded programme on immunization: the immunological basis for immunization. Module 2: diphtheria. WHO document WHO/EPI/GEN/93.12. World Health Organization, Geneva, Switzerland.
3. **Higo-Moriguchi, K., Y. Akahori, Y. Iba, Y. Kurosawa, and K. Taniguchi.** 2004. Isolation of human monoclonal antibodies that neutralize human rotavirus. J. Virol. 78:3325–3332.
4. **Honjo, T., Y. Nishizuka, O. Hayaishi, and I. Kato.** 1968. Diphtheria toxin-dependent adenosine diphosphate ribosylation of aminoacyl transferase II and inhibition of protein synthesis. J. Biol. Chem. 243:3553–3555.
5. **Iba, Y., W. Ito, and Y. Kurosawa.** 1997. Expression vectors for the introduction of highly diverged sequences into the six complementarity-determining regions of an antibody. Gene 194:35–46.
6. **Iwamoto, R., S. Higashiyama, T. Mitamura, N. Taniguchi, M. Klagsbrun, and E. Mekada.** 1994. Heparine-binding EGF-like growth factor, which acts as the diphtheria toxin receptor, forms a complex with membrane protein DRAP27/CD9, which up-regulates functional receptors and diphtheria toxin sensitivities. EMBO J. 13:2322–2330.
7. **Jerne, N. K.** 1951. Study of avidity based on rabbit skin responses to diphtheria toxin-antitoxin mixtures. Acta Pathol. Microbiol. Scand. Suppl. 87:3–183.
8. **Kabat, E. A., T. T. Wu, H. M. Perry, K. S. Gottesman, and C. Foeller.** 1991. Sequences of proteins of immunological interest. National Institutes of Health, Bethesda, Md.
9. **Miyamura, K., S. Nishio, A. Ito, R. Murata, and R. Kono.** 1974. Micro cell culture method for determination of diphtheria toxin and antitoxin titres using VERO cells. I. Studies on factors affecting the toxin and antitoxin titration. J. Biol. Stand. 2:189–201.
10. **Miyamura, K., E. Tajiri, A. Ito, R. Murata, and R. Kono.** 1974. Micro cell culture method for determination of diphtheria toxin and antitoxin titres using VERO cells. II. Comparison with the rabbit skin method and practical application for sero-epidemiological studies. J. Biol. Stand. 2:203–209.
11. **Naglich, J. G., J. E. Metherall, D. W. Russell, and L. Eidels.** 1992. Expression cloning of a diphtheria toxin receptor: identity with a heparin-binding EGF-like growth factor precursor. Cell 69:1051–1061.
12. **Pappenheimer, A. M.** 1977. Diphtheria toxin. Annu. Rev. Biochem. 46:69–94.
13. **Pappenheimer, A. M., T. Uchida, and A. A. Harper.** 1972. An immunological study of the diphtheria toxin molecule. Immunochemistry 9:891–906.
14. **Rolf, J. M., H. M. Gandin, and L. Eidels.** 1990. Localization of diphtheria toxin receptor-binding domain to the carboxyl-terminal M·6000 region of the toxin. J. Biol. Chem. 265:7331–7337.

JVAC6865 1–3

Available online at www.sciencedirect.com

ScienceDirect

Vaccine xxx (2007) xxx–xxx

Vaccine

www.elsevier.com/locate/vaccine

Development of vaccines and passive immunotherapy against SARS corona virus using SCID-PBL/hu mouse models

Masaji Okada [a,*], Yoshinobu Okuno [b], Satomi Hashimoto [a], Yoko Kita [a], Noriko Kanamaru [a], Yasuko Nishida [a], Yoshie Tsunai [a], Ruriko Inoue [a], Hitoshi Nakatani [a], Reiko Fukamizu [a], Yumi Namie [a], Junko Yamada [a], Kyoko Takao [a], Ritsuko Asai [a], Ryoko Asaki [a], Tetsuo Kase [b], Yuji Takemoto [a], Shigeto Yoshida [c], J.S.M. Peiris [d], Pei-Jer Chen [e], Naoki Yamamoto [f], Tatsuji Nomura [g], Isao Ishida [h], Shigeru Morikawa [i], Masato Tashiro [i], Mitsunori Sakatani [a]

[a] *Clinical Research Center, National Hospital Organization, Kinki-Chuo Chest Medical Center, 1180 Nagasone, Kitaku, Sakai, Osaka 591-8555, Japan*
[b] *Department of Infectious Diseases, Osaka Prefectural Institute of Public Health, 3-69 Nakamichi 1-chome Higashinari-ku, Osaka 537-0025, Japan*
[c] *Department of Infection and Immunity, Jichi Medical School, 3311-1 Yakushiji, Minamikawachi-machi, Tochigi 329-0498, Japan*
[d] *Department of Microbiology, The University of Hong Kong, Prokfulam Road, Hong Kong*
[e] *Hapatitis Research Center, National Taiwan University College of Medicine, Room 328, 3F, No. 1, Sec. 1, Ren-ai Rd., Jhongjheng District 100, Taipei, Taiwan*
[f] *AIDS Research Center, National Institute of Infections Diseases, 1-23-1 Toyama, Shinjyuku, Tokyo 162-8640, Japan*
[g] *Central Institute for Experimental Animals, 1430 Nogawa, Miyamae, Kawasaki, Kanagawa 216-0001, Japan*
[h] *Pharmaceutical Frontier Laboratory, Pharmaceutical Division, Kirin Brewery Co., 3 Miyahara, Takasaki, Gunma 370-1295, Japan*
[i] *National Institute of Infectious Diseases, 1-23-1 Toyama, Shinjuku-ku, Tokyo 162-8640, Japan*

Abstract

We have investigated novel vaccine strategies against severe acute respiratory syndrome (SARS) CoV using cDNA constructs encoding the structural antigens: (S), (M), (E), or (N) protein, derived from SARS CoV. PBL from healthy human volunteers were administered i.p. into IL-2 receptor γ-chain disrupted SCID mice, and SCID-PBL/hu mice were constructed. These mice can be used to analyze the human immune response in vivo. SARS M DNA vaccine and N DNA vaccine induced human CTL specific for SARS CoV antigens. Alternatively, SARS M DNA vaccines inducing human neutralizing antibodies and human monoclonal antibodies against SARS CoV are now being developed. These results show that these vaccines can induce virus-specific immune responses and should provide a useful tool for development of protective and therapeutic vaccines.

Keywords: SARS DNA vaccine; SCID-PBL/hu; Human neutralizing antibody against M

1. Introduction

The causative agent of severe acute respiratory syndrome (SARS) has been identified as a new type of corona virus, SARS corona virus (SARS CoV) [1–3]. SARS has infected more than 8400 patients in about 7 months in over 30 countries and caused more than 800 deaths. However, no SARS vaccine is currently available for clinical use. Therefore, we have developed novel vaccine candidates against SARS CoV using cDNA constructs encoding the structural antigens; S, M, E, or N protein. In immunized mice, neutralizing antibodies against the virus and T cell immunity against virus-infected-cells were studied, since these immunities play important roles in protection against SARS CoV and many virus infections. In particular, $CD8^+$ CTL plays an important role in T cell immunity dependent protection against virus infections and the eradication of murine and human cancers [4,5]. In the present study, the SCID-PBL/hu model, which is capable of analyzing in vivo human immune response, was

* Corresponding author. Tel.: +81 72 252 302; fax: +81 72 21 2153.
E-mail address: okm@kch.hosp.go.jp (M. Okada).

0264-410X/$ - see front matter © 2007 Published by Elsevier Ltd.
doi:10.1016/j.vaccine.2007.01.032

Please cite this article in press as: Okada M, et al., Development of vaccines and passive immunotherapy against SARS corona virus using SCID-PBL/hu mouse models, Vaccine (2007), doi:10.1016/j.vaccine.2007.01.032

used because it is a more relevant translational model for human cases [4]. These vaccines induce neutralizing antibody and CTL. This is the first report inducing antibody against SARS M. Theses vaccines should provide useful tool for development of protective vaccines in human.

2. Materials and methods

Three kinds of SARS CoV strains: HKU39849 [1], TW-1 and FFM-1 [2] and their cDNAs were used. S, M, N or E cDNA was transferred into pcDNA 3.1(+) vector [4]. PBL from healthy human volunteers were administered i.p. into IL-2 receptor γ-chain disrupted NOD SCID mice [IL-2R(−/−) NOD-SCID], and SCID-PBL/hu mice were constructed [4]. pcDNA 3.1(+) vector, 50 μg each, containing SARS S, M, N, or E DNA was injected i.m. into SCID-PBL/hu three times, at an interval of 7 days. Neutralizing antibodies against SARS CoV in the serum from the mice were assayed by use of Vero-E6 cell. CTL activity against SARS CoV was studied using human cells, expressing SARS antigens. CTL activity of human CD8-positive lymphocytes in the spleen from SCID-PBL/hu was assessed using 51Cr-release assay [5,6]. Human monoclonal antibodies were produced from B cell hybridoma using P3U1 myeloma cell and spleen cells from human immunoglobulin transchromosomic mice (KM mice) [7].

3. Results

3.1. Induction of human immune responses against SARS CoV using SCID-PBL/hu

The production of neutralizing antibodies against SARS CoV was observed in the serum from mice immunized with S DNA vaccine SARS (M) DNA vaccine and N DNA vaccine induced murine T cell responses against SARS [4]. To analyze the human immune responses, SCID-PBL/hu were constructed and human CD3-positive T lymphocytes and human B cells and macrophages were replaced in the spleen cells and PEC from these SCID-PBL/hu mice, as shown in Fig. 1.

3.2. SARS M DNA vaccine induced the production of human neutralizing antibodies against SARS CoV in SCID-PBL/hu model

Human neutralizing antibodies were induced from SCID-PBL/hu mice vaccines with SARSS [6] and M DNA vaccines (Fig. 2). Titer of neutralizing antibody in the serum from SCID-PBL/hu mice immunized with SARS (M) DNA vaccine was 1:10. In contrast, inhibition of cytopathic effect was observed even in 100-fold dilution of the same serum. Furthermore, B cell hybridoma producing human monoclonal antibodies were established by the fusion of P3U1 cells and

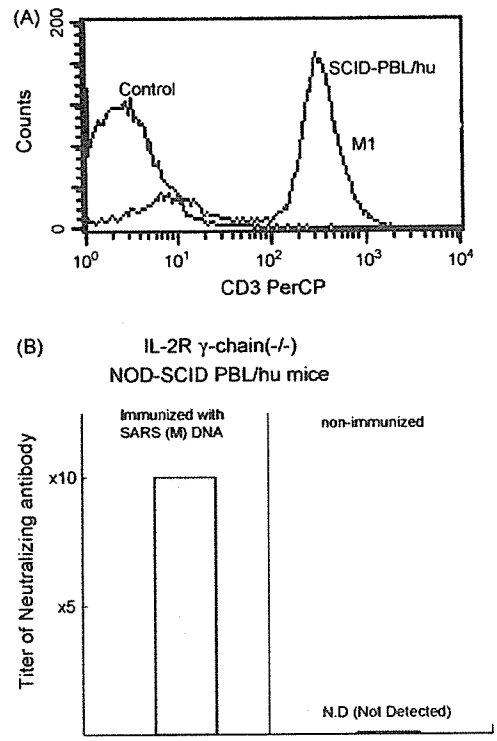

Fig. 1. (A) Human CD3-positive T cells in the spleen from SCID-PBL/hu mice. 1×10^7 PBL from healthy human volunteers were administered i.p. into IL-2R(−/−) NOD-SCID. The number of human CD3-positive T cells were assessed by using anti-human CD3 antibody and FACS. (B) Induction of human neutralizing antibody against SARS coronavirus M protein in SCID PBL/hu mice by SARS (M) DNA vaccination. Titration of neutralizing antibody against SARS CoV in the serum from these mice was assessed by Vero-E6 cells.

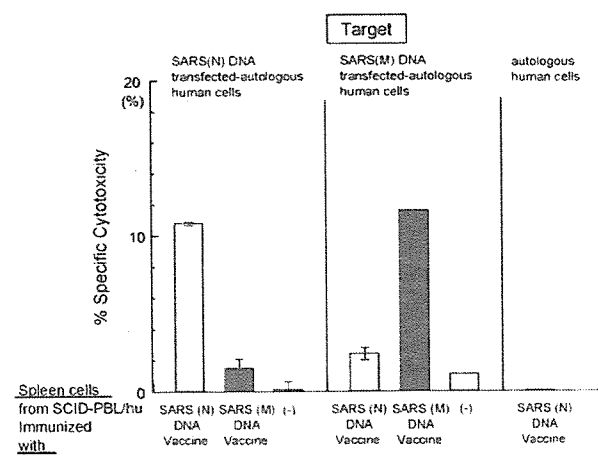

Fig. 2. SARS (N) DNA vaccine and SARS (M) DNA vaccine induces in vivo human CTL against SARS CoV in the SCID-PBL/hu human immune systems. Autologous B blastoid cells transfected with SARS (N) DNA or SARS (M) DNA were used as target cells using ^{51}Cr release assay. E/T ration was 10:1.

Please cite this article in press as: Okada M, et al., Development of vaccines and passive immunotherapy against SARS corona virus using SCID-PBL/hu mouse models, Vaccine (2007), doi:10.1016/j.vaccine.2007.01.032

Table 1
Method for establishment of hybridoma producing human monoclonal antibody against SARS CoV

Humanized monoclonal antibody against SARS-S protein
SARS TW1 strain
S protein (S431-447-KLH)
↓
Human immunoglobulin gene transchromosomic mice (KM mouse)
↓
Spleen + P3U1
↓
Hybridoma (Screening)
Humanized monoclonal antibody against SARS S (431–447) peptide 21 clones

SARS S peptide (S431-447 KLH) was immunized to KM mouse. Hybrid clones producing human monoclonal antibody against SARS S peptide were selected.

spleen cells from human immunoglobulin transchromosomic mice immunized with SARS antigens (Table 1). Specificity is now being studied.

3.3. SARS M DNA and N DNA vaccines induced human T cell immune responses (CTL and proliferation) in SCID-PBL/hu model

The M DNA vaccine enhanced the CTL activity against antologous B blast cells transfected with SARS M DNA but not with SARS N DNA in SCID-PBL/hu mice (Fig. 2). On the other hand, SARS N DNA vaccine augmented the CTL activity specific for autologous B blast cells transfected with SARS N DNA.

4. Discussion

We have demonstrated that SARS (M) DNA and (N) DNA vaccines induce virus-specific immune responses (CTL and T cell proliferation) in the mouse systems using type II lung alveolar T cell lines in clone target models [4]. Gao et al. developed adenovirus based a SARS DNA vaccine encoding S1 polypeptide was capable of inducing neutralizing antibody, while another SARS DNA vaccine encoding N protein generated IFN-γ producing T cells in rhesus monkeys [8]. SARS S DNA vaccine which elicits effective neutralizing antibody responses that generate protective immunity in a mouse model [9]. However its immunogenicity in humans has yet to be established. Therefore, it is very important to evaluate the efficacy of SARS DNA vaccine in a SCID-PBL/hu mice, which is a highly relevant translational model for demonstrating human immune responsiveness.

In the present study, SARS M DNA vaccine and N DNA vaccine induced human CTL specific for SARS M antigen and SARS N antigen, respectively. Furthermore, SARS M DNA as well as SARSS DNA vaccine induce human neutralizing antibodies against SARS CoV by the SCID-PBL/hu model. Antibody against SARS M antigen exerted high inhibitory activity against cytopathic effect by SARS CoV. It was reported that monoclonal antibodies against external domain of M neutralize murine hepatitis corona virus, but only in the presence of complement, and both E and M proteins are required for budding of virions [10]. Neutralizing antibody activity against M protein was not at all eliminated by the inactivation of complement. Antibody against M protein might inhibit the growth of SARS CoV in the cells. Therefore, the effect of combination immunization with such SARS vaccines (M vaccine and S vaccine) and the specificity of human monoclonal neutralizing antibodies are now being studied. These vaccines are expected to provide useful tool for development of therapeutic vaccines.

Acknowledgements

This study was supported by Grant-in-Aid for the science and technology and Grant-in-Aid for Scientific Research on Priority Areas from the Ministry of Education Culture Sports, Science and Technology, Japan. This study also supported by a Heath and Labour Science Research Grant from the Ministry of Health, Labour, and Welfare, Japan.

References

[1] Peiris JS, Lai ST, Poon LL, et al. SARS study group. Coronavirus as a possible cause of severe acute respiratory syndrome. Lancet 2003;361(9366):1319–25.
[2] Drosten C, Gunther S, Preiser W, et al. Identification of a novel coronavirus in patients with severe acute respiratory syndrome. N Engl J Med 2003;348(20):1967–76.
[3] Peiris JS, Yuen KY, Osterhaus AD, Stohr K. The severe acute respiratory syndrome. N Engl J Med 2003;349(25):2431–41.
[4] Okada M, Takemoto Y, Okuno Y, Hashimoto S, Yoshida S, et al. The development of vaccines against SARS corona virus in mice and SCID-PBL-hu mice. Vaccine 2005;23:2269–72.
[5] Tanaka F, Abe M, Akiyoshi T, et al. The anti-human tumor effect and generation of human cytotoxic T cells in SCID mice given human peripheral blood lymphocytes by the in vivo transfer of the Interleukin-6 gene using adenovirus vector. Cancer Res 1997;57(7):1335–43.
[6] Okada M, Yoshimura N, Kaieda T, Yamamura Y, Kishimoto T. Establishment and characterization of human T hybrid cells secreting immunoregulatory molecules. Proc Natl Acad Sci USA 1981;78(12):7717–21.
[7] Ishida I, Tomizuka K, Yoshida H, et al. Production of human monoclonal and polyclonal antibodies in TransChromo (TC) animals. Clon Stem Cells 2002;4:91–102.
[8] Gao W, Tamin A, Soloff A, et al. Effects of a SARS-associated coronavirus vaccine in monkeys. Lancet 2003;362(9399):1895–6.
[9] Yang ZY, Kong WP, Huang Y, et al. A DNA vaccine induces SARS coronavirus neutralization and protective immunity in mice. Nature 2004;428(6982):561–4.
[10] Lai MMC, Holmes KV. Coronaviridae: the viruses and their replication. In: Knipe DM, Howley PM, editors. Fields Virology, vol. 1, 4th ed. Philadelphia: Lippincott Williams & Wilkins; 2001. p. 1163–203.

Please cite this article in press as: Okada M, et al., Development of vaccines and passive immunotherapy against SARS corona virus using SCID-PBL/hu mouse models, Vaccine (2007), doi:10.1016/j.vaccine.2007.01.032

Available online at www.sciencedirect.com
ScienceDirect
Veterinary Microbiology 119 (2007) 121–131
veterinary microbiology
www.elsevier.com/locate/vetmic

A "possible" involvement of TNF-alpha in apoptosis induction in peripheral blood lymphocytes of cats with feline infectious peritonitis

Tomomi Takano, Tsutomu Hohdatsu *, Yoshikiyo Hashida, Yasuhiro Kaneko, Maki Tanabe, Hiroyuki Koyama

Department of Veterinary Infectious Disease, School of Veterinary Medicine and Animal Sciences, Kitasato University, Towada, Aomori 034-8628, Japan

Received 19 April 2006; received in revised form 12 July 2006; accepted 31 August 2006

Abstract

Feline infectious peritonitis (FIP) cats show a decrease in peripheral blood lymphocyte counts, and a particularly marked decrease in T cells including $CD4^+$ and $CD8^+$ cells. In this study, we showed that lymphopenia observed in FIP cats was due to apoptosis, and that the ascitic fluid, plasma, and culture supernatant of peritoneal exudate cells (adherent cells with macrophage morphology, or PEC) from FIP cats readily induced apoptosis in specific pathogen-free cat peripheral blood mononuclear cells, particularly $CD8^+$ cells. In addition, TNF-alpha released from macrophages and TNF-receptor (TNFR) 1 and TNFR2 mRNA expression in lymphocytes were closely involved in this apoptosis induction. In particular, in $CD8^+$ cells cultured in the presence of the PEC culture supernatant, the expression levels of TNFR1 and TNFR2 mRNA were increased, indicating that $CD8^+$ cells are more susceptible to apoptosis induction by TNF-alpha than other lymphocyte subsets, particularly B cells ($CD21^+$ cells). The results of this study suggest that TNF-alpha, produced by virus-infected macrophages, is responsible for induction of apoptosis in uninfected T cells, primarily $CD8^+$ T cells.

Keywords: FIP; Apoptosis; TNF-alpha; TNF-receptor; Lymphopenia; $CD8^+$ cell

1. Introduction

Feline infectious peritonitis (FIP) is a virus-induced, chronic, progressive, usually fatal disease in domestic and wild felines. The causative agent of this disease is feline coronavirus (FCoV). FCoV is mainly composed of nucleocapsid (N) protein, transmembrane (M) protein, and peplomer spike (S) protein (Olsen, 1993), and is classified into types I and II according to S protein properties (Hohdatsu et al., 1991a; Motokawa et al., 1995, 1996). Each of these types consists of two viruses: FIP-causing FIP virus (FIPV)

* Corresponding author. Tel.: +81 176 23 4371; fax: +81 176 23 8703.
E-mail address: hohdatsu@vmas.kitasato-u.ac.jp (T. Hohdatsu).

0378-1135/$ – see front matter © 2006 Elsevier B.V. All rights reserved.
doi:10.1016/j.vetmic.2006.08.033

and non-FIP-causing feline enteric coronavirus (FECV). FIPV and FECV of the same type cannot be distinguished by their antigenicity or at the gene level, and differ only in their pathogenicity for cats.

In the early stage of experimental FIPV infection, general symptoms such as fever, anorexia, vomiting, and diarrhea occur. The development of pathological states after systemic viral dissemination is considered to depend largely on the immune state of the host, particularly the presence or absence of the induction of cell-mediated immunity (TH1 activity): its strong induction inhibits the development of FIP (Pedersen et al., 1984). In cats with overt FIP, the counts of peripheral blood T cells, including $CD4^+$ cells and $CD8^+$ cells, are markedly decreased (De Groot-Mijnes et al., 2005). The induction of humoral immunity (TH2 activity) is considered to be ineffective or rather to aggravate the condition. In the ascitic fluid cells of FIP cats, the production of IL-6, a cytokine involved in the induction of B cell differentiation, is increased (Goitsuka et al., 1990). Antibody production induces immune complexes formation and deposition and a type III hypersensitivity reaction. Recently, Kiss et al. (2004) suggested that immunity against FIP progress is associated with TNF-alpha and IFN-gamma response imbalance, with high TNF-alpha/low IFN-gamma mRNA response favouring disease and low TNF-alpha/high IFN-gamma mRNA responses being indicative of immunity.

The cell/tissue destruction in FIPV lesion is mainly due to tissue reaction with activation of type III (tissue destroyed by enzymes released by polymorphonuclear neutrophil leukocytes) or IV (cell-mediated cytotoxicity) hypersensitivity (Kipar et al., 1998; Pedersen, 1987). On the contrary, lymphocyte depletion and the presence of apoptotic cells were reported to be detected in the T-cell region of mesenteric lymph nodes and the spleen of FIP cats (Haagmans et al., 1996). Dean et al. (2003) reported that the FIPV antigen, TNF-alpha expression, and lymphocyte depletion were colocalized in the lymphoid tissues of FIP cats. Haagmans et al. (1996) reported that anti-human TNF-alpha did not inhibit apoptosis induced by ascitic fluid from FIPV-infected cats. Thus, the detailed mechanism of apoptosis induction in the lymphoid tissue of FIP cats remains unclear. As described above, FIP cats show a marked reduction in peripheral blood lymphocyte counts. Since FIPV does not replicate in peripheral blood lymphocytes, it is difficult to consider this lymphopenia to be due to direct destruction by virus infection of lymphocytes, leaving the causes unknown. Since the development of FIP is closely related to the immune function of the host, clarification of the mechanism of lymphopenia is important for elucidating the pathogenesis of FIP.

In this study, we showed that lymphopenia in FIP cats was due to apoptosis, and that TNF-alpha released from macrophages of FIP cats induced apoptosis in lymphocytes, particularly $CD8^+$ T cells.

2. Materials and methods

2.1. Experimental animals

FIPV strain 79-1146 (10^4 $TCID_{50}$/ml) was administered orally to 6–8-month-old, specific pathogen-free (SPF) cats. Nine cats that developed FIP symptoms (FIP cats), such as fever, weight loss, peritoneal or pleural effusion, dyspnea, ocular lesions, and neural symptoms, six cats infected but resistant to the development of disease (FIPV-infected non-FIP cats), and eight 6–8-month-old SPF cats as controls were used in this study.

2.2. Cell cultures

Feline peripheral blood mononuclear cells (PBMC), $CD4^+$ cells, $CD8^+$ cells, $CD21^+$ cells, peritoneal exudate cells (PEC), alveolar macrophages, and WEHI-164 murine sarcoma cells were maintained in RPMI 1640 growth medium supplemented with 10% FCS, antibiotics, 50 μM 2-mercaptoethanol, and 2 μg/ml of polybrene. WEHI-164 murine sarcoma cells (ATCC CRL1751) were obtained from the American Type Culture Collection.

2.3. Separation of PBMC

Heparinized blood (10 ml) was two-fold diluted with phosphate-buffered saline (PBS), and subjected to Ficoll-Hypaque density gradient centrifugation at 1700 rpm for 20 min. The PBMC layer was collected, washed twice with PBS, and resuspended with growth medium at 2×10^6 cells/ml.

2.4. Specimens from FIP cats and FIP-infected non-FIP cats

Blood collected from FIP cats and FIP-infected non-FIP cats using a heparinized syringe was centrifuged at 3000 rpm for 10 min, and the supernatant was used as a plasma sample. As for ascitic fluid samples, ascitic fluid was collected from FIP cats using a heparinized syringe and centrifuged at 3000 rpm for 10 min, and the supernatant was collected.

2.5. Recovery of PEC and alveolar macrophages

PEC were collected from the ascitic fluid of FIP cats. The cell pellet, obtained by centrifugation of the effusion collected from the FIP cats, was washed three times with Hank's balanced salt solution (HBSS), and suspended in growth medium at a density of 2×10^6 cells/ml. One milliliter of the cell suspension was placed into each well of a 24-well plate, and cultured at 37 °C for 2 h. The culture supernatant was discarded, the non-adherent cells were removed by washing with HBSS, and the remaining cells were used as PEC.

Feline alveolar macrophages were obtained by bronchoalveolar lavage with HBSS from coronavirus antibody-negative SPF cats, as previously described by Hohdatsu et al. (1991b).

2.6. Separation of $CD8^+$, $CD4^+$, and $CD21^+$ cells

To separate $CD8^+$ cells, PBMC (1×10^7 cells) were incubated with 500 μl of purified monoclonal antibody (MAb) OKT8 (ATCC CRL8014) IgG at 4 °C for 30 min. MAb OKT8 recognizes the alpha-chain of human CD8 antigen and cross-reacts with feline $CD8^+$ cells (Hohdatsu et al., 1998; Pecorado et al., 1994). The cells were washed three times with PBS containing 2 mM EDTA and 0.5% BSA, 40 μl of microbeads coated with rat anti-mouse IgG2a+b (Miltenyi Biotec, Germany) were added to the cells, and the mixture was incubated at 4 °C for 15 min. After washing with PBS containing 2 mM EDTA and 0.5% BSA, the cells were fractionated into $CD8^+$ cells and $CD8^+$-depleted cells by a magnetic system using a MACS kit (Miltenyi Biotec, Germany). $CD4^+$ and $CD21^+$ cells were recovered using MAb fCD4 (Southern Biotechnology Associates, USA) or MAb CA2.1D6 IgG (Serotec Ltd., UK) as a primary antibody, and microbeads coated with rat anti-mouse IgG1 (Miltenyi Biotec, Germany) as a secondary antibody in the same manner as that for $CD8^+$ cells.

The purity of the cell population was 92.0 ± 1.6% (mean ± S.D.) for $CD8^+$ cells, 93.3 ± 3.8% for $CD4^+$ cells and 96.9 ± 0.8% for $CD21^+$ cells, respectively.

2.7. Apoptosis-inducing activities of FIP cat-derived specimens on peripheral $CD4^+$, $CD8^+$, and $CD21^+$ cells

PBMC, $CD4^+$ cells, $CD8^+$ cells and $CD21^+$ cells (2×10^6 cells) were cultured for 4 h in the presence of FIP cat-derived ascitic fluid (final concentration of 1:40), plasma (final concentration of 1:40), culture supernatant of PEC (final concentration of 1:2), and FIPV-infected non-FIP cats-derived plasma (final concentration of 1:40), and were examined for their apoptosis-inducing activities. Culture supernatants of PEC were prepared by culturing cells (2×10^6 cells/ml) recovered from ascitic fluids for 24 h. Apoptosis induction was detected by the TUNEL method using flow cytometric analysis.

2.8. Detection of apoptosis by TUNEL

A total of 2×10^6 cells were washed twice, resuspended in 200 μl of PBS, and fixed by adding an equal volume of 4% formaldehyde for 20 min at room temperature. The cells were washed once again with PBS, suspended in cell permeability buffer (0.5% saponin, 0.5% BSA, and 0.1% sodium azide in PBS), and incubated for 15 min in the dark. The fixed and permeabilized cells were washed twice with PBS containing 0.5% BSA and 0.1% sodium azide, and incubated with terminal deoxynucleotidyl transferase (TdT) and FITC-dideoxyuridine triphosphate (dUTP) at 37 °C for 1 h. Negative controls were incubated in the absence of TdT. After rinsing the cells with PBS containing 0.5% BSA and 0.1% sodium azide, the fluorescence intensity was measured using a FACS 440 cell sorter (Becton Dickinson, USA).

2.9. Apoptosis inhibitors

SB203580, Z-DEVD-FMK, and Z-IETD-FMK were used as apoptosis inhibitors. SB203580, a specific

inhibitor of p38 mitogen-activated protein kinase (p38-MAPK), was purchased from Promega Corporation (USA). Z-DEVD-FMK (caspase-3 inhibitor) and Z-IETD-FMK (caspase-8 inhibitor) were purchased from Medical Biological Laboratories Corporation (Japan).

2.10. RNA isolation and cDNA preparation

Total cellular RNA was extracted from PBMC, PEC, and macrophages using a High Pure RNA Isolation Kit (Roche Diagnostics, Switzerland) according to the instructions of the manufacturer. RNA was dissolved in elution buffer.

Using total cellular RNA as a template, cDNA was synthesized using Ready-to-Go RT-PCR beads (GE Healthcare Life Sciences, USA). Reverse transcription was performed in a 50 μl final volume containing 0.5 μg oligo(dT)$_{12-18}$ primers. The resulting solution was incubated at 42 °C for 1 h to synthesize cDNA.

2.11. Determination of levels of feline GAPDH, TNF-alpha, TNFR1, and TNFR2 mRNA expression

cDNA was amplified by PCR using specific primers for feline GAPDH, TNF-alpha, TNFR1, and TNFR2. The primer sequences are shown in Table 1.

PCR was performed in a total volume of 50 μl. One microliter of sample cDNA was mixed with 10-fold concentrated reaction buffer (TaKaRa, Japan), 4 μl of deoxynucleotide mix (TaKaRa, Japan) containing 2.5 mM each, 2 μl of 20 μM primer mix, 0.25 μl of Ex Taq polymerase (1000 U; Takara, Japan), and 37.75 μl of distilled water. Using a PCR Thermal Cycler Dice (Takara, Japan), the DNA was amplified at 94 °C for 5 min, followed by 35 cycles of denaturation at 94 °C for 30 s, primer annealing at 55 °C for 45 s, and synthesis at 72 °C for 45 s, with a final extension at 55 °C for 5 min. The PCR products were resolved by electrophoresis on 2% agarose gels. The gels were incubated with SYBR Green I Nucleic Acid Gel Stain (Roche Diagnostics, Switzerland), and bands were visualized using a UV transilluminator at 312 nm and photographed.

Band density was quantified under appropriate UV exposure by video densitometry using Scion Image software (Scion Corporation, USA).

To quantify TNF-alpha, TNFR1, and TNFR2 mRNA were quantitatively analyzed in terms of the relative density value to the mRNA for the housekeeping gene GAPDH.

2.12. Cytotoxic activity against TNF-alpha using WEHI-164 cells

WEHI-164 cells were grown to confluence in growth medium at 37 °C. The cells were detached with trypsin, washed in fresh medium, seeded into 96-well plates at a density of 10^5 cells/well in 100 μl of fresh medium, and allowed to adhere for 4 h at 37 °C. The medium was then aspirated, and 100 μl (10 μg/ml) of actinomycin D sulfate (Sigma–Aldrich, USA) were added to each well. Samples to be tested were diluted in medium, and 100 μl of each dilution was added to triplicate wells. The plates were incubated at 37 °C for 2 h. The culture supernatants were removed, and 100 μl of fresh medium were added to each well. After incubation at 37 °C for 12 h, 10 μl of WST-8 solution (WST-8 cell proliferation assay kit; Kishida Chemical Co. Ltd., Japan) were added, and the cells were

Table 1
Sequences of PCR primers for feline GAPDH, TNF-alpha, and TNF receptors

	Orientation	Nucleotide sequence	Location	Length (bp)	Reference
GAPDH	Forward	5′-AATTCCACGGCACAGTCAAGG-3′	158–78	97	Avery and Hoover (2004)
	Reverse	5′-CATTTGATGTTGGCGGGATC-3′	235–254		
TNF-alpha	Forward	5′-TGGCCTGCAACTAATCAACC-3′	195–214	251	Avery and Hoover (2004)
	Reverse	5′-GTGTGGAAGGACATCCTTGG-3′	426–445		
TNFR1	Forward	5′-CGAAGTGCCACAAAGGGACCTAC-3′	388–411	215	Mizuno et al. (2001)
	Reverse	5′-TGGTTCTTCCTGCAGCCACACAC-3′	579–601		
TNFR2	Forward	5′-CTCAGGCAGCACCGCAGACGG-3′	1–21	244	Mizuno et al. (2001)
	Reverse	5′-GCCGGAGGAGCTGGCATCCACG-3′	226–247		

returned to the incubator for 1 h. The absorbance of formazan produced was measured at 450 nm with a 96-well spectrophotometric plate reader, as described by the manufacturer. The percent cytotoxicity was calculated by the following formula: cytotoxicity (%) = (negative control OD – test sample OD/negative control OD) × 100.

2.13. Statistical analysis

Data were analyzed by Student's *t*-test. The data in Fig. 1 were also analyzed by the Mann–Whitney test. *p*-Values < 0.05 were considered to indicate a significant difference between compared groups.

3. Results

3.1. Detection of apoptosis in PBMC of FIP cats and FIPV-infected non-FIP cats

Using PBMC of FIP cats and experimentally FIPV-infected non-FIP cats, apoptotic cells were detected by TUNEL, and the rates of apoptosis were compared with that in SPF cats. The blood lymphocyte counts at the time of blood sampling are shown in Fig. 1A. The blood lymphocyte counts in SPF cats, FIP cats and FIPV-infected non-FIP cats were 5177 ± 731 μl^{-1} (mean ± S.D.), 1100 ± 924 μl^{-1}, and 4850 ± 1780 μl^{-1}, respectively (Fig. 1A). The rate of apoptosis in the PBMC of FIP cats was significantly higher, at 23.4 ± 16.7% (mean ± S.D.), than that in non-FIP cats (0.9 ± 1.3%) and SPF cats (2.5 ± 2.8%) (Fig. 1B).

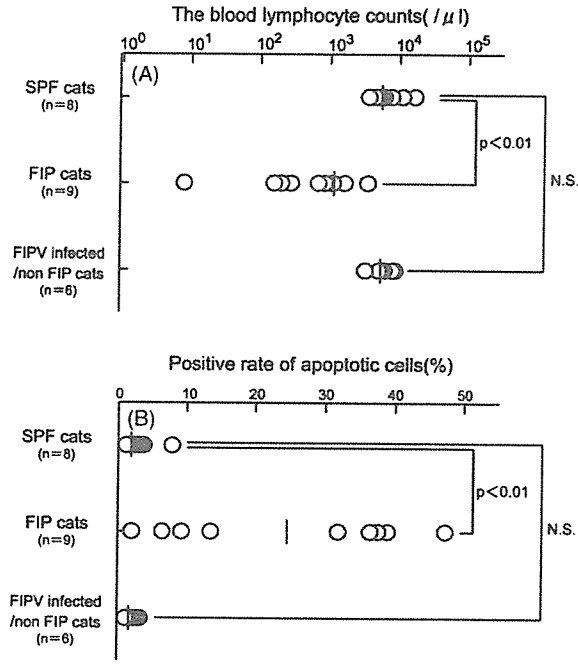

Fig. 1. (A) The blood lymphocyte counts of FIP cats and FIP-infected non-FIP cats. (B) Detection of apoptotic cells in PBMC of FIP cats and FIP-infected non-FIP cats. PBMC were recovered from SPF cats, FIP cats, and FIP-infected non-FIP cats, and apoptotic cells were detected by TUNEL. Horizontal lines represent the median for each group. N.S. indicates not significant.

3.2. Apoptosis-inducing activities of FIP cat-derived specimens on peripheral $CD4^+$, $CD8^+$, and $CD21^+$ cells

All FIP cat-derived specimens readily induced apoptosis in PBMC and their subsets of $CD4^+$, $CD8^+$, and $CD21^+$ cells (Fig. 2), significantly more strongly in $CD8^+$ than in $CD21^+$ cells ($p < 0.01$ for ascitic fluid and PEC supernatant, $p < 0.05$ for plasma of FIP cats). A significant difference was noted in the apoptosis-inducing activity of PEC supernatant between $CD4^+$ and $CD8^+$ cells ($p < 0.05$).

We examined whether inhibitors of intracellular apoptotic signal transduction (caspase-3 inhibitor, caspase-8 inhibitor, and p38-MAPK inhibitor) inhibited the apoptosis-inducing activities of ascitic fluid and PEC culture supernatant in the PBMC of SPF cats. As a result, all these inhibitors inhibited apoptosis induction in a dose-dependent manner (Fig. 3).

3.3. Determination of levels of TNF-alpha mRNA expression in PEC and PBMC of FIP cats and detection of TNF-alpha in their PEC culture supernatant and plasma

Since TNF-alpha is known as an apoptosis inducer, the levels of TNF-alpha mRNA expression were determined in the PEC of FIP cats, alveolar macrophages of SPF cats and FIPV-infected non-FIP cats, and PBMC of FIP cats, SPF cats and FIPV-infected non-FIP cats.

The level of TNF-alpha mRNA expression was markedly increased in the PEC of FIP cats ($n = 7$), and was significantly higher than that in the alveolar macrophages of SPF cats ($n = 6$) and FIPV-infected non-FIP cats ($n = 3$) ($p < 0.01$). Similar results were

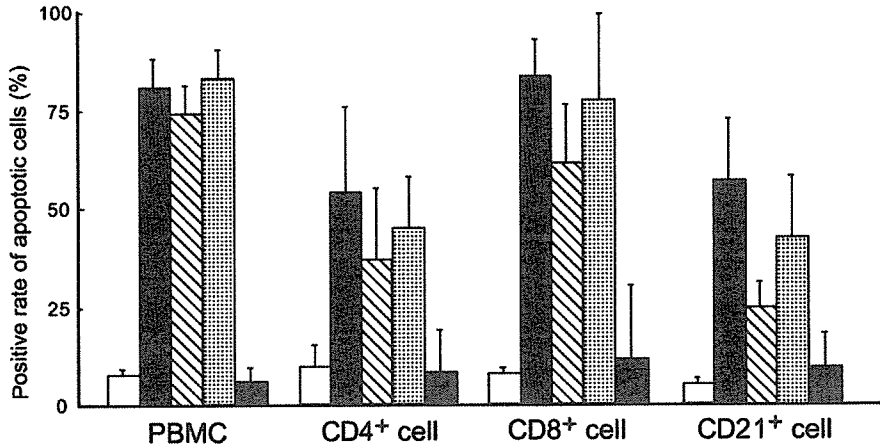

Fig. 2. Apoptosis-inducing activities of specimens from FIP cats in peripheral blood $CD4^+$, $CD8^+$, and $CD21^+$ cells. The PBMC (2×10^6) of SPF cats and their subsets of lymphocytes $CD4^+$, $CD8^+$, and $CD21^+$ cells (2×10^6) were cultured at 37 °C for 4 h in the presence of the ascitic fluid, PEC culture supernatant, or plasma of FIP cats, and apoptotic cells were detected by TUNEL. $CD4^+$, $CD8^+$, and $CD21^+$ cells were recovered with magnetic beads. Medium (white), ascitic fluid of FIP cats (gray), culture supernatant of PEC from FIP cats (oblique), plasma of FIP cats (dot), plasma of FIP-infected non-FIP cats (black).

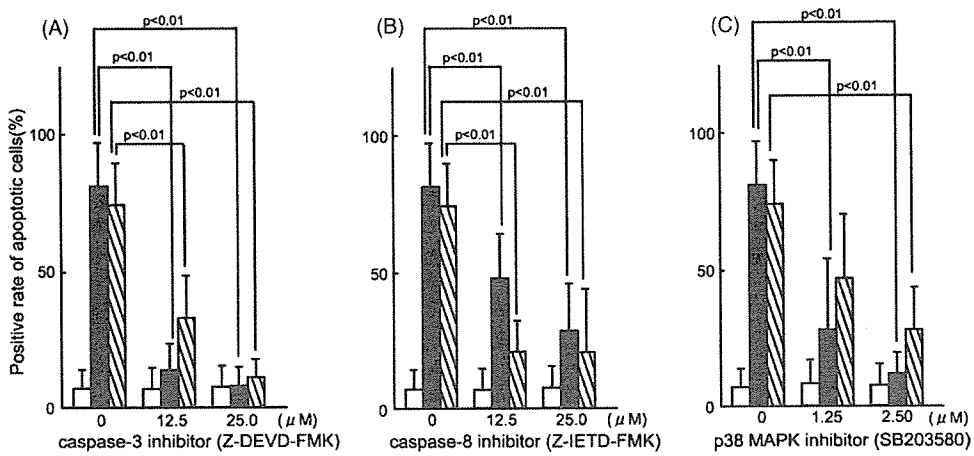

Fig. 3. Effects of inhibitors of intracellular apoptotic signal transduction on apoptosis in PBMC. (A and B) The PBMC of SPF cats were incubated for 2 h with caspase-3 inhibitor (A) or caspase-8 inhibitor (B), and cultured at 37 °C in the presence of the ascitic fluid or culture supernatant of PEC from FIP cats. Four hours later, apoptotic cells were detected by TUNEL. (C) The PBMC of SPF cats were cultured at 37 °C for 1 h in the presence of the ascitic fluid or culture supernatant of PEC from FIP cats, and p38-MAPK inhibitor was added. After further culture for 3 h, apoptotic cells were detected by TUNEL. Medium (white), ascitic fluid of FIP cats (gray), culture supernatant of PEC from FIP cats (oblique).

obtained for TNF-alpha mRNA expression in PBMC, and the expression level was significantly higher in the FIP cats than in the SPF cats and FIPV-infected non-FIP cats (Fig. 4A).

We examined the plasma and culture supernatant of PEC from FIP cats for TNF-alpha using its cytotoxic activity against TNF-alpha-sensitive WEHI-164 cells. As a result, the plasma and culture supernatant of PEC from FIP cats exhibited cytotoxic activity against WEHI-164 cells in a dose-dependent manner, whereas alveolar macrophages and plasma SPF cats did not (Fig. 4B).

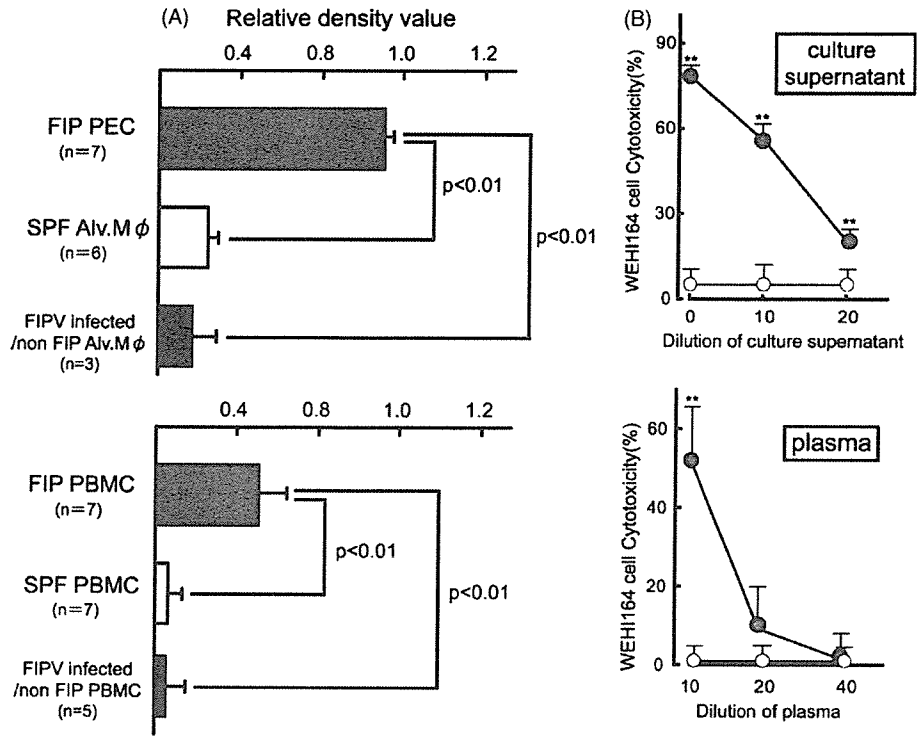

Fig. 4. Determination of TNF-alpha mRNA expression in PEC and PBMC of FIP cats and TNF-alpha in their PEC culture supernatant and plasma. (A) The PEC of FIP cats, alveolar macrophages of SPF cats and FIPV-infected non-FIP cats, and PBMC of FIP cats, SPF cats, and FIPV-infected non-FIP cats were recovered, and TNF-alpha mRNA expression levels were measured. TNF-alpha mRNA was quantitatively analyzed in terms of the relative density value to the mRNA for the housekeeping gene GAPDH. (B) Using the culture supernatant of the PEC of FIP cats or macrophages of SPF cats, and the plasma of FIP or SPF cats, TNF-alpha was measured using the rate of cytotoxicity against WEHI-164 cells as an indicator. Specimens from FIP cats (gray circle), or SPF cats (white circle). $^{**}p < 0.01$ vs. SPF cats.

3.4. Analysis of TNFR1 and TNFR2 mRNA expression in PBMC of SPF cats

Since TNF-alpha binds to cell surface TNF-receptor (TNFR) 1 and TNFR2 to induce apoptosis and cell proliferation, we compared the levels of TNFR1 and TNFR2 mRNA expression in the PBMC of FIP cats, SPF cats and FIPV-infected non-FIP cats. As a result, the levels of TNFR1 and TNFR2 mRNA expression in PBMC were higher in FIP cats than in SPF cats and FIPV-infected non-FIP cats (Fig. 5).

3.5. In vitro effects of culture supernatant of PEC from FIP cats on the expression of TNFR1 and TNFR2 mRNA in PBMC

The PBMC of SPF cats were cultured in the presence of the culture supernatant of FIP cat-derived

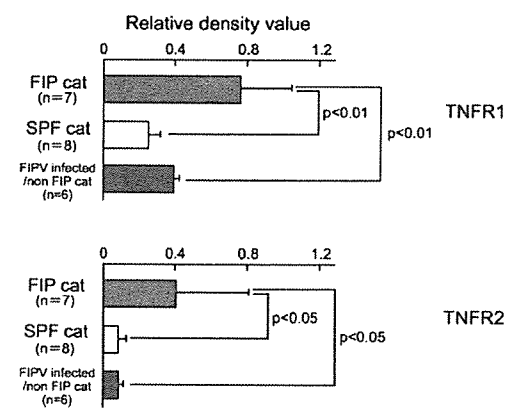

Fig. 5. Analysis of TNF-receptor mRNA production in PBMC. The PBMC of SPF cats, FIP cats, or FIPV-infected non-FIP cats were recovered, and the levels of TNFR1 and TNFR2 mRNA expression were measured. TNFR1 and TNFR2 mRNA were quantitatively analyzed in terms of the relative density value to the mRNA for the housekeeping gene GAPDH.

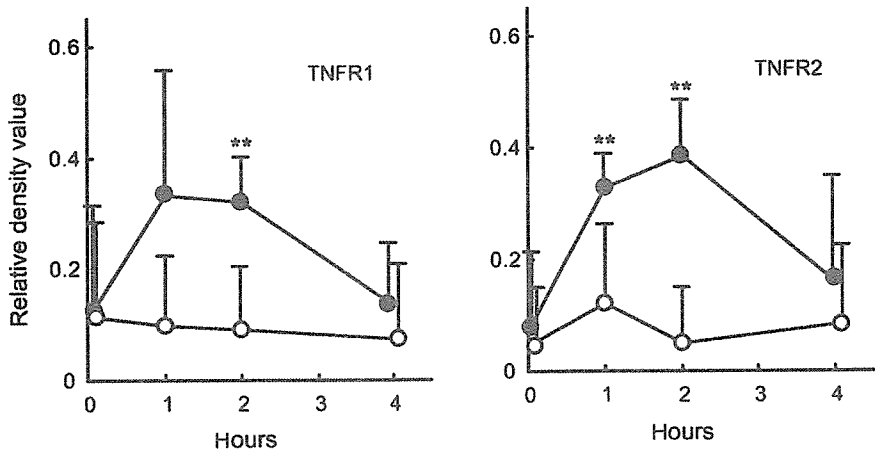

Fig. 6. *In vitro* effects of the culture supernatant of PEC from FIP cats on the expression of TNFR1 and TNFR2 mRNA in PBMC. The PBMC of SPF cats ($n = 5$) were cultured in the presence of the culture supernatant of PEC from FIP cats, and the levels of TNFR1 and TNFR2 mRNA expression were measured 0, 1, 2, and 4 h after culture. The levels of TNFR1 and TNFR2 mRNA expression were quantitatively analyzed in terms of the relative density value to the mRNA for the housekeeping gene GAPDH. The culture supernatant of PEC from FIP cats (gray circle), medium (white circle). $^{**}p < 0.01$.

PEC, and TNFR1 and TNFR2 in PBMC were measured sequentially. As a result, both TNFR1 and TNFR2 mRNA increased from 1 h after culture, and decreased at 4 h (Fig. 6).

In addition, the effects of the culture supernatant of PEC from FIP cats on the expression of TNFR1 and TNFR2 mRNA in $CD4^+$, $CD8^+$, and $CD21^+$ cells separated from the PBMC of SPF cats were examined. When $CD4^+$, $CD8^+$, or $CD21^+$ cells were cultured for 2 h in the presence of the supernatant of PEC, the levels of TNFR1 and TNFR2 mRNA expression increased in $CD4^+$ and $CD8^+$ cells, but remained unchanged in $CD21^+$ cells (Fig. 7).

4. Discussion

Lymphocyte apoptosis has been detected in the lymph nodes and spleen of FIP cats (Haagmans et al., 1996; Kipar et al., 2001), but not in peripheral blood lymphocytes. This study appears to be the first to directly demonstrate that lymphopenia in FIP cats is due to apoptosis. Lymphocyte apoptosis in the lymph nodes and spleen of FIP cats may be associated with peripheral blood lymphocyte apoptosis; however, it has been reported that in SIV or influenza virus infection (Rosenberg et al., 1993; Tumpey et al., 2000), the rate of apoptosis in the spleen and lymph nodes is not correlated with that in peripheral blood lymphocytes. By comparing the rates of apoptosis in the spleen, lymph nodes, and peripheral blood lymphocytes, it should be further investigated whether apoptosis induction in lymphoid tissue is reflected in peripheral blood lymphocytes in FIPV infection.

The detailed mechanism of apoptosis induction in the lymphoid tissues of FIP cats is not clear. FIPV does not replicate in lymphocytes, suggesting that this apoptosis in lymphocytes is not directly induced by FIPV infection, but indirectly by other factors. In this study, we showed that: (1) the levels of TNF-alpha mRNA expression was increased in the PEC and PBMC of FIP cats, (2) the PEC culture supernatant and plasma of FIP cats showed cytotoxic activity against TNF-alpha-sensitive WEHI-164 cells, and (3) the ability of the ascitic fluid and PEC culture supernatant of FIP cats to induce apoptosis in the PBMC of SPF cats was inhibited by caspase-3, caspase-8, and p38-MAPK inhibitors, suggesting that apoptosis in the lymphocytes of FIP cats is mainly induced by TNF-alpha. These results support the report of Dean et al. (2003) that lymphocyte depletion and TNF-alpha expression were colocalized in the lymphoid tissues of FIP cats. However, Haagmans et al. (1996) reported that anti-human TNF-alpha did not inhibit apoptosis-induced by ascitic fluid from FIP-infected cats, which was inconsistent with our

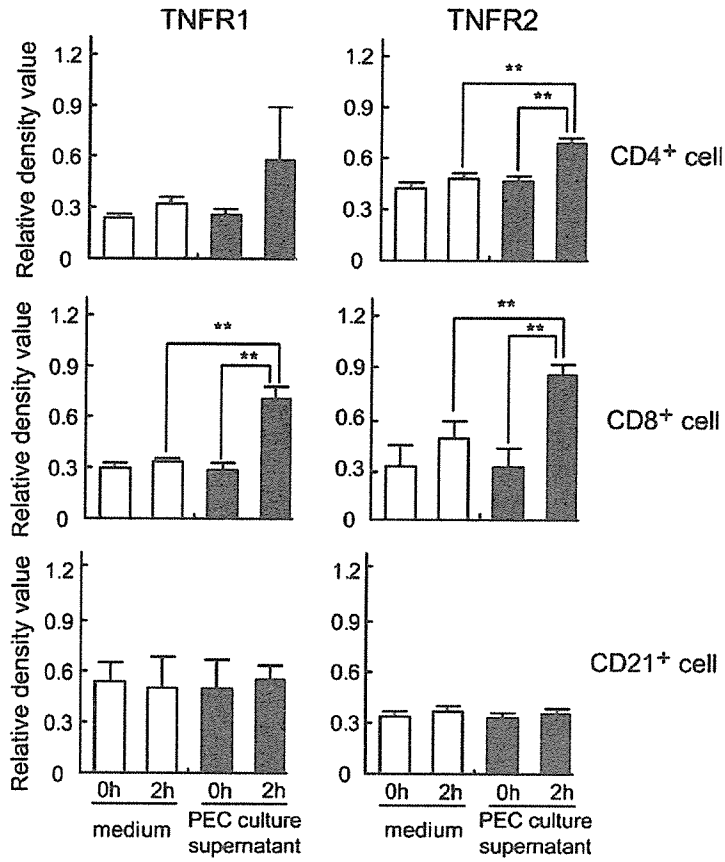

Fig. 7. *In vitro* effects of the culture supernatant of macrophages from FIP cats on the expression of TNFR1 and TNFR2 mRNA in $CD4^+$, $CD8^+$, and $CD21^+$ cells. $CD4^+$, $CD8^+$, and $CD21^+$ cells were recovered from the PBMC of SPF cats using magnetic beads, and cultured in the presence of the culture supernatant of PEC from FIP cats. The levels of TNFR1 and TNFR2 mRNA expression were measured 0 and 2 h after culture. The levels of TNFR1 and TNFR2 mRNA expression were quantitatively analyzed in terms of the relative density value to the mRNA for the housekeeping gene GAPDH. $^{**}p < 0.01$.

results and those of Dean et al. (2003). Although the cause of this discrepancy is not clear, experiments using anti-feline TNF-alpha antibodies are expected.

The ascitic fluid of FIP cats contains cells such as macrophages, lymphocytes, and neutrophils, all of which produce TNF-alpha. In this study, we used PEC containing adherent cells, obtained after removing non-adherent cells present in the ascitic fluid. These adherent cells had the morphology of macrophages, and the FIPV gene was detected in them by RT-PCR. The macrophage is one of the target cells of FIPV, and FIPV infection of macrophages is considered to be an important factor in the progression of FIP (Rottier et al., 2005; Stoddart and Scott, 1989). Thus, we speculate that FIPV-infected macrophages produce TNF-alpha, which induces apoptosis in lymphocytes, particularly $CD8^+$ T cells. Further studies are needed to investigate the relationship of the macrophage tropism of FIPV with the production of TNF-alpha and with the induction of apoptosis in lymphocytes.

TNF-alpha binds to TNFR to induce an apoptotic signal in cells (Herbein and O'Brien, 2000). Two types of TNFR are known to exist: TNFR1 has a death domain, and is directly involved in the induction of apoptosis (Herbein and O'Brien, 2000), whereas TNFR2 has no death domain, but assists in apoptosis-inducing signal transduction (Chan and Lenardo, 2000; Fotin-Mleczek et al., 2002). In this study, we showed that the levels of TNFR1 and TNFR2 mRNA expression were increased in the PBMC of FIP cats and

the PBMC of SPF cats that had been cultured in the presence of the PEC culture supernatant, suggesting that the induction of apoptosis in the lymphocytes of FIP cats is closely associated with TNF-alpha. In particular, in $CD8^+$ cells, the levels of TNFR1 and TNFR2 mRNA expression were increased, suggesting that $CD8^+$ cells are more susceptible to apoptosis induction by TNF-alpha than other subsets of lymphocytes. The rate of apoptosis induction in $CD21^+$ cells (B cells) by specimens from FIP cats was lower than those in $CD8^+$ and $CD4^+$ cells. Goitsuka et al. (1990) reported that IL-6 activity was increased in the ascitic fluid and PEC culture supernatant of FIP cats. IL-6 is known to be involved in the differentiation and proliferation of B cells and the inhibition of apoptosis (Dolcetti and Boiocchi, 1996; Liu et al., 1994; Moreno et al., 2001; Tumang et al., 2002). Therefore, the low rate of apoptosis induction in $CD21^+$ cells suggests the influence of IL-6 contained in specimens from FIP cats. In $CD21^+$ cells cultured in the presence of the PEC culture supernatant, the levels of TNFR1 and TNFR2 mRNA expression remained unchanged, also suggesting that IL-6 is involved in the rate of apoptosis induction by TNF-alpha. At present, it is not clear why the levels of TNFR mRNA expression increase in $CD8^+$ and $CD4^+$ cells cultured in the presence of the PEC culture supernatant. Further studies are needed to investigate the relationship between T-cell apoptosis induction and TNFR in FIP cats.

It is also possible that apoptosis-inducing factors other than TNF-alpha, such as Fas ligand and TRAIL, are involved in lymphocyte apoptosis in FIP cats, for which further investigation is necessary. Currently, we are investigating the relationship between lymphocyte apoptosis induction and the Fas ligand in FIP cats. The involvement of not only the death receptor pathway investigated but also the mitochondrial pathway should be investigated as an apoptosis induction pathway.

The above results suggest that, in FIP cats, TNF-alpha produced by FIPV-infected macrophages induces apoptosis in lymphocytes, particularly $CD8^+$ cells, resulting in decreased cell-mediated immunity. Comparative analysis of mRNA expression levels of TNFR showed that $CD8^+$ cells are particularly susceptible to apoptosis induction. The results of this study will aid understanding of the role of TNF-alpha in T-cell apoptosis and resultant lymphopenia in FIP diseased cats.

Acknowledgment

This work was supported by Ministry of Health, Labor, and Welfare Grant H16-Shinkoh-9.

References

Avery, P.R., Hoover, E.A., 2004. Gamma interferon/interleukin 10 balance in tissue lymphocytes correlates with down modulation of mucosal feline immunodeficiency virus infection. J. Virol. 78, 4011–4019.

Chan, F.K., Lenardo, M.J., 2000. A crucial role for p80 TNF-R2 in amplifying p60 TNF-R1 apoptosis signals in T lymphocytes. Eur. J. Immunol. 30, 652–660.

Dean, G.A., Olivry, T., Stanton, C., Pedersen, N.C., 2003. In vivo cytokine response to experimental feline infectious peritonitis virus infection. Vet. Microbiol. 97, 1–12.

De Groot-Mijnes, J.D., Van Dun, J.M., Van der Most, R.G., De Groot, R.J., 2005. Natural history of a recurrent feline coronavirus infection and the role of cellular immunity in survival and disease. J. Virol. 79, 1036–1044.

Dolcetti, R., Boiocchi, M., 1996. Cellular and molecular bases of B-cell clonal expansions. Clin. Exp. Rheumatol. 14, 3–13.

Fotin-Mleczek, M., Henkler, F., Samel, D., Reichwein, M., Hausser, A., Parmryd, I., Scheurich, P., Schmid, J.A., Wajant, H., 2002. Apoptotic crosstalk of TNF receptors: TNF-R2-induces depletion of TRAF2 and IAP proteins and accelerates TNF-R1-dependent activation of caspase-8. J. Cell Sci. 115, 2757–2770.

Goitsuka, R., Ohashi, T., Ono, K., Yasukawa, K., Koishibara, Y., Fukui, H., Ohsugi, Y., Hasegawa, A., 1990. IL-6 activity in feline infectious peritonitis. J. Immunol. 144, 2599–2603.

Haagmans, B.L., Egberink, H.F., Horzinek, M.C., 1996. Apoptosis and T-cell depletion during feline infectious peritonitis. J. Virol. 70, 8977–8983.

Herbein, G., O'Brien, W.A., 2000. Tumor necrosis factor (TNF)-alpha and TNF receptors in viral pathogenesis. Proc. Soc. Exp. Biol. Med. 223, 241–257.

Hohdatsu, T., Okada, S., Koyama, H., 1991a. Characterization of monoclonal antibodies against feline infectious peritonitis virus type II and antigenic relationship between feline, porcine, and canine coronaviruses. Arch. Virol. 117, 85–95.

Hohdatsu, T., Nakamura, M., Ishizuka, Y., Yamada, H., Koyama, H., 1991b. A study on the mechanism of antibody-dependent enhancement of feline infectious peritonitis virus infection in feline macrophages by monoclonal antibodies. Arch. Virol. 120, 207–217.

Hohdatsu, T., Okubo, M., Koyama, H., 1998. Feline $CD8^+$ T cells non-cytolytic anti-feline immunodeficiency virus activity mediated by a soluble factor(s). J. Gen. Virol. 79, 2729–2735.

Kipar, A., Bellmann, S., Kremendahl, J., Kohler, K., Reinacher, M., 1998. Cellular composition, coronavirus antigen expression and production of specific antibodies in lesions in feline infectious peritonitis. Vet. Immunol. Immunopathol. 65, 243–257.

Kipar, A., Kohler, K., Leukert, W., Reinacher, M., 2001. A comparison of lymphatic tissues from cats with spontaneous feline

infectious peritonitis (FIP), cats with FIP virus infection but no FIP, and cats with no infection. J. Comp. Pathol. 125, 182–191.

Kiss, I., Poland, A.M., Pedersen, N.C., 2004. Disease outcome and cytokine responses in cats immunized with an avirulent feline infectious peritonitis virus (FIPV)-UCD1 and challenge-exposed with virulent FIPV-UCD8. J. Feline Med. Surg. 6, 89–97.

Liu, J., Li, H., de Tribolet, N., Jaufeerally, R., Hamou, M.F., Van Meir, E.G., 1994. IL-6 stimulates growth and inhibits constitutive, protein synthesis-independent apoptosis of murine B-cell hybridoma 7TD1. Cell. Immunol. 155, 428–435.

Mizuno, T., Goto, Y., Baba, K., Masuda, K., Ohno, K., Tsujimoto, H., 2001. TNF-alpha induced cell death in feline immunodeficiency virus-infected cells is mediated by the caspase cascade. Virology 287, 446–455.

Moreno, A., Villar, M.L., Cámara, C., Luque, R., Cespón, C., González-Porqué, P., Roy, G., López-Jiménez, J., Bootello, A., Santiago, E.R., 2001. Interleukin-6 dimers produced by endothelial cells inhibit apoptosis of B-chronic lymphocytic leukemia cells. Blood 97, 242–249.

Motokawa, K., Hohdatsu, T., Aizawa, C., Koyama, H., Hashimoto, H., 1995. Molecular cloning and sequence determination of the peplomer protein gene of feline infectious peritonitis virus type I. Arch. Virol. 140, 469–480.

Motokawa, K., Hohdatsu, T., Hashimoto, H., Koyama, H., 1996. Comparison of the amino acid sequence and phylogenetic analysis of the peplomer, integral membrane and nucleocapsid proteins of feline, canine and porcine coronaviruses. Microbiol. Immunol. 40, 425–433.

Olsen, C.W., 1993. A review of feline infectious peritonitis virus: molecular biology, immunopathogenesis, clinical aspects, and vaccination. Vet. Microbiol. 36, 1–37.

Pecorado, M.R., Kawaguchi, Y., Miyazawa, T., Norimine, J., Maeda, K., Toyosaki, T., Tohya, Y., Kai, C., Mikami, T., 1994. Isolation, sequence and expression of a cDNA encoding the alpha-chain of the feline CD8. Immunology 81, 127–131.

Pedersen, N.C., 1987. Virologic and immunologic aspects of feline infectious peritonitis virus infection. Adv. Exp. Med. Biol. 218, 529–550.

Pedersen, N.C., Black, J.W., Boyle, J.F., Everman, J.F., Mckeirnan, A.J., Ott, R.I., 1984. Pathogenic differences between various feline coronavirus isolates. Adv. Exp. Med. Biol. 173, 365–380.

Rosenberg, Y.J., Zack, P.M., White, B.D., Papermaster, S.F., Elkins, W.R., Eddy, G.A., Lewis, M.G., 1993. Decline in the CD41 lymphocyte population in the blood of SIV-infected macaques is not reflected in lymph nodes. AIDS Res. Hum. Retrov. 9, 639–646.

Rottier, P.J., Nakamura, K., Schellen, P., Volders, H., Haijema, B.J., 2005. Acquisition of macrophage tropism during the pathogenesis of feline infectious peritonitis is determined by mutations in the feline coronavirus spike protein. J. Virol. 79, 14122–14130.

Stoddart, C.A., Scott, F.W., 1989. Intrinsic resistance of feline peritoneal macrophages to coronavirus infection correlates with in vivo virulence. J. Virol. 63, 436–440.

Tumang, J.R., Hsia, C.Y., Tian, W., Bromberg, J.F., Liou, H.C., 2002. IL-6 rescues the hyporesponsiveness of c-Rel deficient B cells independent of Bcl-xL, Mcl-1, and Bcl-2. Cell. Immunol. 217, 47–57.

Tumpey, T.M., Lu, X., Morken, T., Zakim, S.R., Katzm, J., 2000. Depletion of lymphocytes and diminished cytokine production in mice infected with a highly virulent influenza A (H5N1) virus isolated from humans. J. Virol. 74, 6105–6116.